ACS APPLIED MATERIALS & INTERFACES

www.acsami.org

Research Article

Macroporous Silicone Chips for Decoding Microbial Dark Matter in Environmental Microbiomes

Ahmed E. Zoheir, Laura Meisch, Marta Velaz Martín, Christoph Bickmann, Alexei Kiselev, Florian Lenk, Anne-Kristin Kaster, Kersten S. Rabe, and Christof M. Niemeyer*

Cite This: *ACS Appl. Mater. Interfaces* 2022, 14, 49592–49603

Read Online

ACCESS | Metrics & More | Article Recommendations | Supporting Information

ABSTRACT: Natural evolution has produced an almost infinite variety of microorganisms that can colonize almost any conceivable habitat. Since the vast majority of these microbial consortia are still unknown, there is a great need to elucidate this "microbial dark matter" (MDM) to enable exploitation in biotechnology. We report the fabrication and application of a novel device that integrates a matrix of macroporous elastomeric silicone foam (MESIF) into an easily fabricated and scalable chip design that can be used for decoding MDM in environmental microbiomes. Technical validation, performed with the model organism *Escherichia coli* expressing a fluorescent protein, showed that this low-cost, bioinert, and widely modifiable chip is rapidly colonized by microorganisms. The biological potential of the chip was then illustrated through targeted sampling and enrichment of microbiomes in a variety of habitats ranging from wet, turbulent moving bed biofilters and wastewater treatment plants to dry air-based environments. Sequencing analyses consistently showed that MESIF chips are not only suitable for sampling with high robustness but also that the material can be used to detect a broad cross section of microorganisms present in the habitat in a short time span of a few days. For example, results from the biofilter habitat showed efficient enrichment of microorganisms belonging to the enigmatic *Candidate Phyla Radiation*, which comprise ~70% of the MDM. From dry air, the MESIF chip was able to enrich a variety of members of *Actinobacteriota*, which is known to produce specific secondary metabolites. Targeted sampling from a wastewater treatment plant where the herbicide glyphosate was added to the chip's reservoir resulted in enrichment of *Cyanobacteria* and *Desulfobacteria*, previously associated with glyphosate degradation. These initial case studies suggest that this chip is very well suited for the systematic study of MDM and opens opportunities for the cultivation of previously unculturable microorganisms.

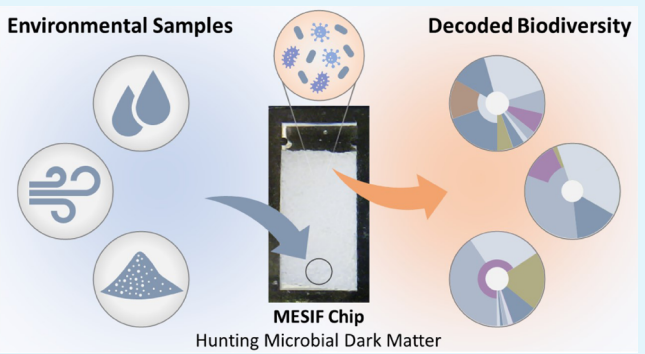

KEYWORDS: *microbial dark matter, biodiversity, selective enrichment, silicon foams, PDMS, chips, microfabrication*

1. INTRODUCTION

In the course of billions of years of evolution, nature has created a myriad of microorganisms that can conquer almost any conceivable habitat by forming complex communities. The vast majority of these microbial consortia are, however, uncharacterized and cannot be cultured in the laboratory. Modern methods of high-throughput nucleic acid sequencing are beginning to allow us to better understand the enormous complexity of this so-called "microbial dark matter".[1] However, although a surprisingly large number of branches are already visible, the full extent of the microbial tree of life is still difficult to imagine.[2] This lack of knowledge is critical, as it is becoming increasingly clear that microbial communities not only play an important role in human health and our environment[3] but could also serve as invaluable tools for the next generation of biotechnological processes.[4] Therefore, there is a growing interest in efficient strategies to isolate novel microorganisms from complex habitats to exploit the biological materials and information they contain, for example, specific proteins or metabolic pathways, for biotechnological applications.[5]

To improve the accessibility of noncultivable microorganisms for technical cultivation, the so-called "isolation chip" (ichip) platform had been developed to isolate previously noncultivable microorganisms from environmental samples by allowing exposure to natural growth factors through in situ cultivation.[6] To achieve this, cultivation was moved to the microbes' natural habitat by placing cells taken from various environmental samples into miniaturized diffusion chambers of a chip, which was then returned to the natural habitat for

Received: August 28, 2022
Accepted: October 7, 2022
Published: October 26, 2022

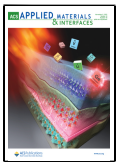

https://doi.org/10.1021/acsami.2c15470
ACS Appl. Mater. Interfaces 2022, 14, 49592–49603

incubation. Although the ichip platform can increase microbial biomass from, for example, soil samples by 5- to 300-fold, the technology is cumbersome because environmental samples must first be collected, then processed for integrating single cells into the chip, and the chips thus processed must be reincubated in the original habitat. Hence, it is difficult to sample, for example, aqueous and/or dynamic habitats, such as moving bed biofilters or wastewater treatment plants (WWTP).

We here report a novel approach for chip-based isolation of microorganisms in which a macroporous, elastomeric silicone foam (MESIF) is used as a matrix for colonization and isolation of microorganisms from arbitrary habitats. The MESIF matrix can be manufactured on a large scale, offers ideal wetting and diffusion properties, can be chemically tailored with respect to its surface properties, and is easily integrated into selection chips available via soft-lithographic fabrication. The resulting MESIF chips are mechanically robust and resilient, making them applicable in a wide range of very challenging, complex habitats that include dry, wet, and liquid environments, such as indoor air, soils, moving bed biofilters, or WWTP. We demonstrate that the macroporous silicone foam matrix is colonized by microorganisms surprisingly quickly and efficiently, such that after a few days of incubation in diverse environmental habitats, a stable population is formed within the matrix that can be identified using next-generation sequencing. Since the chip can be easily loaded with solid, liquid, and gaseous substances that influence microbial colonization, it can also be used for the targeted enrichment of microorganisms.

2. EXPERIMENTAL SECTION

2.1. Preparation of MESIF Materials and Chips. *2.1.1. MESIF Material Preparation.* MESIF material and chips were produced following the workflow sketched in Figures S1 and S2. Initially, a two-part casting mold (Figure S2A) was designed using Autodesk Inventor software 2020 (Autodesk Inc., USA) and milled with a CNC micromilling machine (Mini Mill GX, Minitech Machinery, USA). The two parts of the mold were closed by nine screws. The porogen used was sodium chloride table salt (ChanteSel iodized salt fine from Lidl, Germany), the particles of which were fractionated using a sieve with the following inserts: 25 mesh (707 μm), 35 mesh (500 μm), 45 mesh (354 μm), 60 mesh (250 μm), and 80 mesh (177 μm). The resultant porogen fractions were weighed individually and the ratio to the mass of the sieved salt was calculated to estimate the mass fractions.

To prepare the polydimethylsiloxane (PDMS) prepolymer, a silicone elastomer was mixed with a curing agent (Sylgard 184, Down Corning) in a ratio of 10:1, respectively, then degassed in a vacuum chamber for 1 h. Liquid PDMS prepolymer (0.9 mL) was poured inside the closed mold to fill approximately half of its volume and the remaining free volume was filled with table salt porogen of the desired particle size. The filled mold was centrifuged (5804 R, Eppendorf) at 4600 rpm and 4 °C for 20 min to disperse and pack the porogen crystals within the liquid PDMS prepolymer. After centrifugation, the PDMS−porogen mixture was cured in an oven (Heraeus, Thermo Scientific Inc.) at 70 °C for 1 h, then the mold screws were removed, and the solid, casted PDMS−porogen mixture piece was carefully released from the mold as a single piece (~65 × 10 × 3 mm^3) as shown in Figure S2C.

To leach the porogen from the cured PDMS−porogen, the released piece was repeatedly pressed by hand in a 50 °C water bath until the material reached a soft, elastic, and sponge-like structure. To remove all salt residues, the material was stirred overnight in a beaker filled with 250 mL of ddH_2O at 40 °C and washed the next morning with fresh ddH_2O. The resultant MESIF material was then dried at 90 °C for 1 h in the oven and then cut into pieces of ~18 × 10 × 3 mm^3 (Figure S2D) using a scalpel. These final MESIF pieces fit into the MESIF chip housing structure (Figure S2G).

2.1.2. MESIF Chip Production. To produce the MESIF chip, a casting mold corresponding to the housing structure was designed using Autodesk Inventor software (Figure S2E) and milled on a poly(methyl methacrylate) (PMMA) plate using a CNC micromilling machine. To cast the housing structure, PDMS prepolymer was prepared as described above and poured into the chip mold and then cured at 70 °C for 1 h in the oven. After curing, the cast was peeled off the mold and was ready to fit the MESIF material pieces inside (Figure S2F). Likewise, a mold for the chip cover lid (76 × 26 × 0.75 mm^3) was prepared using the same procedure into which the holes (ø 4 mm) for the environmental contacts were manually inserted with a press puncher.

For assembling the MESIF chip, the prepared three components (MESIF piece, PDMS housing, and lid) were individually activated by plasma treatment (Plasma Flecto10, PlasmaTechnology) for 30 s at 300 W and 0.2 mbar. Then, the MESIF piece was placed in the corresponding empty space in the PDMS housing, covered with the PDMS lid (Figure S2H) and the assembled chip was cured at 90 °C for 30 min for permanent bonding.

2.2. Characterization. *2.2.1. Material and Porogen Morphology.* The morphology of the MESIF material was investigated with environmental scanning electron microscopy (ESEM). To visualize the pore structure and morphology within the MESIF material, it was cut into ~1 mm thick layers with a scalpel, then coated with 1.5 nm platinum and examined using ESEM at 20 kV under vacuum. The software ImageJ was used for further analysis of the acquired images. By setting a gray threshold and manual post-processing, all pores were colored black and separated from each other and evaluated using ImageJ's "Analyze Particle" function. Porogen crystals and respective sieved fractions were examined by ESEM and analyzed by ImageJ using the same method to calculate the size distribution and mass fraction percentage.

2.2.2. Diffusion Experiment. The interconnectivity of the pores as well as the diffusion behavior within the MESIF chip were investigated with the help of the fluorescent model solute 5-carboxyfluorescein (λ_{Exc} = 492 nm, λ_{Em} = 517 nm). A stock solution of the dye (100 mM in dimethyl sulfoxide) was stored in a −20 °C freezer, and a dilution of 10 μM in ddH_2O was freshly prepared upon use.

Chips with different MESIF pore sizes were filled with ddH_2O, which was injected into the chip reservoir with a syringe and perfused through the MESIF matrix until it exited the environmental contact hole. At least 1 mL of ddH_2O was injected into the chip to ensure that the MESIF matrix was completely soaked. The filled chips were then placed in a Petri dish with the environmental contact holes facing upward, then 40 μL of 10 μM 5-carboxyfluorescein solution was loaded onto the contact hole. Five milliliters of ddH_2O was added to the Petri dish to ensure adequate humidity. The dish lid was closed and sealed with parafilm to prevent the chips from drying. The Petri dish was kept at room temperature in the dark for the entire experiment to avoid photobleaching. To determine the diffusion progress, images of the Petri dish were taken over the experimental time using a fluorescence gel imager (Fusion FX, Vilber) at an exposure time of 1 ms. At least three independent chips were used in these experiments.

For microbial growth in the MESIF chip, a lab stock *Escherichia coli* DH5α strain[7] transformed with a plasmid bearing a kanamycin selection marker gene and arabinose-inducible red fluorescent protein (*E. coli*-RFP) was used. A preculture of 5 mL of Lysogeny Broth (LB) medium (10 g L^{-1} tryptone, 5 g L^{-1} yeast extract, 10 g L^{-1} NaCl, all dissolved in ddH_2O and autoclaved) supplemented with 50 μg mL^{-1} kanamycin and 10 mM arabinose was inoculated with *E. coli*-RFP and incubated overnight at 37 °C in a 180 rpm shaker. This preculture (20 μL) was loaded onto the contact hole of MESIF chips, previously autoclaved at 121 °C for 20 min and prefilled with LB medium containing 50 μg mL^{-1} kanamycin and 10 mM arabinose, using the same method explained above. The inoculated chips were then placed

https://doi.org/10.1021/acsami.2c15470
ACS Appl. Mater. Interfaces 2022, 14, 49592−49603

in a sterile Petri dish, and 5 mL of ddH_2O was added to the Petri dish to ensure humidity. The Petri dish was sealed with parafilm and incubated at 37 °C for the respective incubation times. The growth progress indicated by red fluorescence was documented using a gel imager. At least three independent chips were used.

To investigate the diffusion of the fluorescent dye as well as the growth of *E. coli*-RFP inside the MESIF matrix in the chip, an automated fluorescence analysis method was used, as detailed in Figure S3. Over the course of the experiments, grayscale images (Figure S3A) were collected at defined time intervals with the Fusion FX fluorescence gel imager under identical instrument settings.

2.3. Chemical Surface Modification. *2.3.1. Surface Activation.* To activate the surface of the MESIF materials, the protocol developed by Sui et al. was used.[8] In brief, MESIF materials were immersed in the activation solution composed of ddH_2O, concentrated H_2O_2 (30% v/v), and concentrated HCl (37% v/v) in a volume ratio of 5:1:1 at room temperature. In the activating solution, the materials were mechanically squeezed by hand for 2 min, followed by stirring in the same solution for 3 min. This procedure was repeated five times. Afterward, the MESIF materials were washed with ddH_2O until a neutral pH value in the washing water was achieved. Finally, the materials were dried overnight in an oven at 90 °C.

2.3.2. Functionalization of the Activated Surface. Three different surface functionalization methods were used to install amino-, epoxy-, or polyethyleneglycol (PEG) groups on the MESIF surface using (3-aminopropyl) triethoxysilane (APTES, Sigma-Aldrich) (Figure S4A), (3-glycidyloxypropyl) trimethoxysilane (GPTS, Sigma-Aldrich) (Figure S4B), or a PDMS-polyethyleneglycol (PDMS-PEG) block copolymer (Figure S4C). Modification with APTES and GPTS (Figure S4D,E) was achieved by following the method of Yu et al.[9] In brief, the surface-activated MESIF materials were heated in a solution of toluene containing the appropriate organosilane (2% v/v) at 80 °C for 24 h to obtain the desired surface functionalization. The materials were then washed with toluene and dichloromethane and any solvent residues were removed at 40 °C and under reduced pressure.

2.3.3. Acidic Ring-Opening of GPTS-Functionalized MESIF to Generate GPTSo-MESIF. To open the epoxy ring of the GPTS (Figure S4E-II), GTPS-functionalized MESIF materials were immersed in a 1:1 mixture of concentrated HCl (37% v/v) and ddH_2O. The materials were mechanically squeezed by hand for 25 min in the acidic solution to open the epoxide to the corresponding diol. Afterward, the MESIF pieces were washed with ddH_2O until a neutral pH value was reached in the washing solution. The pieces were then dried overnight in an oven at 90 °C.

2.3.4. Functionalization with PEG Copolymer. PDMS prepolymer and thermal curing agent were mixed in a ratio of 9:1 as a polymerization mixture. Additionally, a PDMS-PEG block copolymer (Gelest Inc.) was added in a ratio of 0.25% (w/w), to introduce PEG units into the material (Figure S4C,F). The resulting PDMS prepolymer solution was then used to prepare MESIF materials as described above in Section 2.1.1.

2.3.5. Coupling of DNA Oligonucleotides to GPTS-Functionalized MESIF. To couple DNA oligonucleotides to the surface of GPTS-functionalized MESIF (Figure S5), MESIF pieces were incubated in 3 mL of phosphate buffered salt solution (PBS) containing 100 nm of the DNA oligonucleotide AmC12Tr12-Cy5 (5′-amine-C_{12}-T_8-$(ATG)_4$-Cy5-3′). The MESIF pieces were shaken in the solution for 6 h, at room temperature and at 175 rpm. To improve mass transport inside the MESIF, the pieces were squeezed manually with a glass rod every 0.5 h for 1 min. Following, the MESIF pieces were washed five times with PBS, and each time the MESIF materials were squeezed with a glass rod for 1 min. Removal of unbound DNA was monitored by UV/vis absorbance measurements of the washing solution.

For hybridization of the DNA-functionalized MESIF, the pieces were incubated in 3 mL of PBS containing 100 nM complementary oligomer Cy3-cTr12 (5′-Cy3-$(CAT)_4$-3′). Incubation was done under shaking for 6 h at room temperature at 175 rpm and repeated squeezing every 0.5 h with a glass rod. The pieces were then washed five times with PBS, and the UV/vis absorbance of the washing solution was measured. The so-treated MESIF was then examined to accurately localize DNA within the pore structure using confocal laser scanning microscopy (CLSM, ZEISS LSM 880, Carl Zeiss Inc.). Excitation wavelengths and filters for Cy5 (λ_{Exc} = 633 nm, λ_{Em} = 666 nm) and Cy3 (λ_{Exc} = 561 nm, λ_{Em} = 568 nm) and by transmitted light were used as shown in Figure S5. The successful hybridization and thus formation of double-stranded DNA was confirmed via Förster resonance energy transfer (FRET) with Cy5-excitation and measured with Cy3-emission (λ_{Exc} = 561 nm, λ_{Em} = 666 nm). This analysis was applied to DNA-modified MESIF before and after hybridization.

2.4. Microbial Growth and Sampling Studies. *2.4.1. Sampling of Microorganisms from the Moving Bed Biofilter.* The MESIF material ability to enrich microorganisms from the moving bed biofilter of a fish farm, compared to commercial biofilter support chips made of polyethylene (MUTAG BioChip, Multi Umwelttechnologie AG, Germany), was investigated. MESIF pieces (10 × 10 × 3 mm^3) prepared with unsieved porogen and MUTAG chips (ø 300 mm) were sterilized by autoclaving at 121 °C for 20 min. Sterile MESIFs and MUTAGs were then incubated free-floating in the biofilter tank for 18 days, then collected, briefly washed with ddH_2O, and frozen at −20 °C for temporary storage and transport. Duplicate MUTAG chips and MESIF pieces were used.

2.4.2. Sampling of Airborne Microorganisms. Sterile MESIF chips in an adapted setup were used to enrich airborne microorganisms in open air inside an indoor poultry farm containing 2 chickens per m^2. The adapted device as shown in Figure 5A comprised a MESIF chip filled with LB cultivation medium and connected from the side of the reservoir to 1 mL syringe through a needle (both from B-Braun GmbH). A 0.2 μm sterile syringe filter was plugged into the other side of the syringe to allow for ventilation. The syringe was filled with LB medium to serve as an extended reservoir for the chip, enabling wet conditions and continued viable cultivation. Chips with the environmental contact hole facing upward were placed on top of a 2 m high cabinet inside the poultry farm and incubated for 9 days, and then collected and stored at −20 °C until further analysis. As a control, 1 mL of LB medium in open 1.5 mL sterile Eppendorf tubes was incubated at the same conditions. Triplicate MESIF chips and control Eppendorf tubes were used.

2.4.3. Sampling of Microorganisms from Chemical Wastewater. To test the MESIF chip for its ability to selectively enrich on the herbicide glyphosate, chips were prepared with unsieved porogen salt and autoclaved as described above. Native chemical wastewater medium, collected from the wastewater treatment facility of Karlsruhe Institute of Technology, was autoclaved and supplemented with 8 g L^{-1} glyphosate (Monsanto, Bayer). Sterile chips were then filled with native wastewater medium and loaded in duplicates inside a 50 mL falcon tube in which multiple pores were manually drilled to enable inflow of environmental wastewater. Control chips but without glyphosate addition were prepared under identical conditions. The Falcon tubes were then loaded into a metal rack and immersed ∼40 cm deep inside a static chemical wastewater collection tank in the open air and left for 6 days. The chips were then collected and gently washed with sterile ddH_2O followed by storage at 20 °C until further analysis. Duplicate MESIF chips with or without glyphosate were used.

2.5. Sequencing and Bioinformatic Analysis. Genomic DNA (gDNA) was extracted from the sampling MESIF chips described above. Under sterile conditions, the MESIF matrix was removed from the chip, then was cut into small pieces using a sterile scalpel (Figure S6A) and collected in a 2 mL sterile Eppendorf tube. The commercial Quick-DNA Miniprep Plus Kit (Zymo Research GmbH, Germany) was used to extract the gDNA from the MESIF according to the manufacturer's protocol. The concentration of extracted gDNA was subsequently quantified photometrically by NanoDrop OneC Microvolume and fluorometrically by Qubit 3 (both from Thermo Scientific Inc.).

From the purified gDNA, the 16S rRNA V3 region was amplified using the degenerate primers 341bf (ACACTCTTTCCCTACACGACGCTCTTCCGATCTCCTACGGGNGGCWGCAG) and 518r

https://doi.org/10.1021/acsami.2c15470
ACS Appl. Mater. Interfaces 2022, 14, 49592−49603

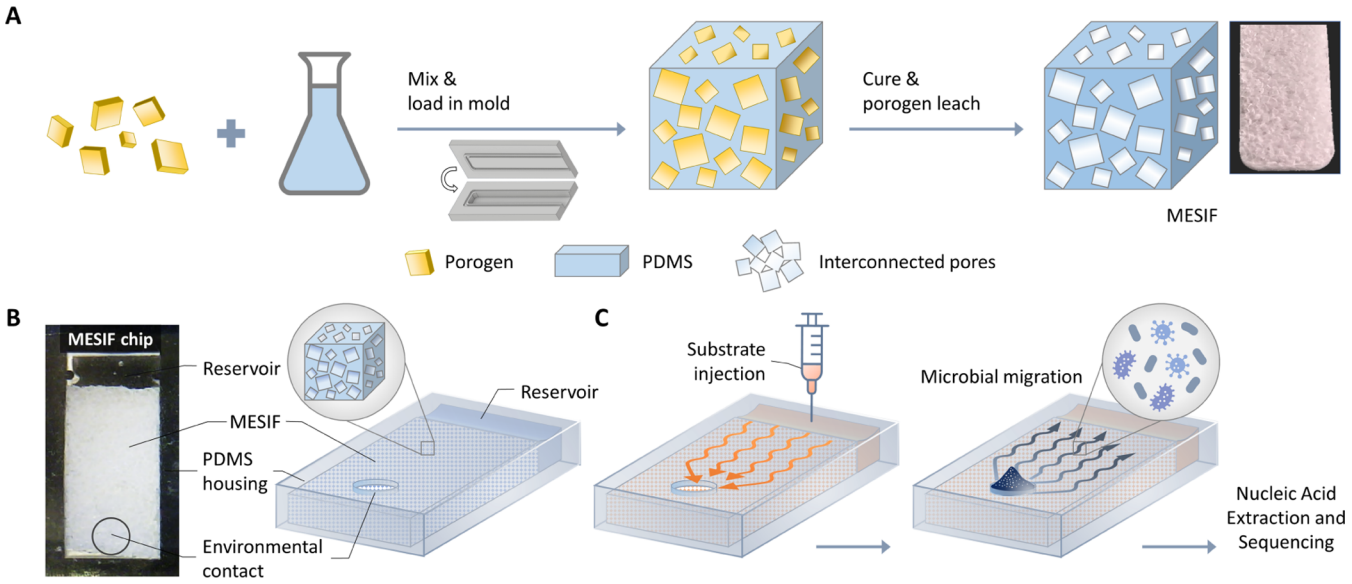

Figure 1. MESIF material preparation and chip concept. (A) Workflow of MESIF material preparation by mixing the porogen (sodium chloride) with PDMS prepolymer solution. The mixture is then molded and cured, followed by porogen leaching to yield the macroporous, elastomeric silicone foam (MESIF). (B) Integration of the MESIF material into a precast PDMS chip, and (C) use of the chip for targeted enrichment of microbial communities. A culture medium or growth substrate is injected into the reservoir, filling the entire MESIF matrix. Insertion of the chip into the habitat to be sampled allows microbial communities in the isolation sample to enter the contact hole and spread within the MESIF matrix toward the nutrients in the reservoir. After incubation is complete, the chip is recovered from the habitat and DNA can be extracted from the MESIF matrix and subsequently sequenced.

(GACTGGAGTTCAGACGTGTGCTCTTCCGATCTWTTACCGCRGCTGCTGG), which include Illumina TruSeq adapter sequences. The PCR reactions contained 0.04 U μL^{-1} High-Fidelity Q5 DNA Polymerase, 1 × Q5 reaction buffer, 1 × high GC enhancer, 0.25 μM of each primer, 0.2 mM dNTPs, and 100 ng template DNA in a total reaction volume of 25 μL. Amplification was carried out using a touchdown protocol with the following cycling conditions (95 °C, 2 min; 4 × [95 °C, 9 s; 56−52 °C, 40 s; 72 °C, 40 s] 25 × [95 °C, 40 s; 51 °C, 40 s; 72 °C, 40 s]; 72 °C, 5 min; hold at 8 °C).

Indexed sequencing libraries were constructed from the purified product by the NEBNext Ultra II FS DNA Library Prep Kit (New England BioLabs, Germany), using the protocol for input amounts ≥100 ng and beginning with the size selection step. Unique dual indices (NEB, Germany) were added in six cycles of an index PCR. DNA library quality was verified using the Agilent High Sensitivity DNA Kit on the Agilent 2100 Bioanalyzer instrument (Agilent Technologies, Germany). Paired-end reads were generated on an Illumina NextSeq 550 (Illumina, USA) with the NextSeq 500/550 High Output Kit v2.5 (300 Cycles) (Illumina, USA).

Adapter sequences and low-quality reads were removed using Trimmomatic, version 0.39, with the ILLUMINACLIP (2:30:10), SLIDINGWINDOW (4:15), MINLEN (80), and LEADING and TRAILING (both 3) options.[10] The remaining reads were further trimmed with BBDuk, version 38.73 (ktrim = r, mink = 11, minlength = 80, entropy = 0.25), and Cutadapt, version 1.18 (-a "AGATCGG$," -a "CCGATCT$").[11,12] The high-quality paired-end reads were merged using FLASH, version 1.2.11 (15 ≤ overlap ≤ 100, maximum 5% mismatches).[13] OTU tables were compiled in four steps with the program vsearch, version 2.17.1.[14] First, the reads were dereplicated (--derep_fulllength) and singletons were removed (--minuniquesize 2). They were then clustered at 97% identity and the cluster centroid sequences were reported. Chimeras were detected and removed with the --uchime_denovo option, and finally, reads were mapped back onto the centroids via the -usearch_global option and output as OTU tables. The centroid sequences were aligned to the SILVA SSU reference database for taxonomic classification.[15] The results were visualized as KRONA charts.[16]

3. RESULTS AND DISCUSSION

3.1. Fabrication of Macroporous Elastomeric Silicone Foam (MESIF) Chips. Bacterial communities colonize nearly all available wet habitats, many of which are characterized by porous topography, hydrophilic, and hydrophobic surfaces.[17,18] Based on previous work on culturing biofilms on PDMS surfaces,[19−21] we hypothesized that this material might be ideal for isolation of microbes when provided as a porous support matrix. Although a variety of hydrophobic micro-, meso-, or macroporous materials exist, PDMS has the unique advantages of being biochemically inert, easy to process, and modifiable in terms of its surface properties through well-controlled silane chemistry. In addition, the production of foam- and sponge-like porous silicone has been well studied, and it has already been shown that these materials can be used for applications as oil absorbers, heterogeneous catalysts, actuators, and sensors, or even for tissue engineering of animal cells.[22]

To produce MESIF chips, we used the method of Wessling and colleagues[23] sketched in Figure 1A. Briefly, sodium chloride crystals were used as porogens by first mixing the crystals with a prepolymer solution and pouring the resulting suspension into a casting mold made of PMMA. After thermal curing at 70 °C for 1 h, the resulting molded body was mechanically compressed several times in a water bath to dissolve the integrated porogen and thereby create a macroporous structure of interconnected pores within the elastomer. For a detailed illustration of the workflow, see Figures S1 and S2.

For assembly of the MESIF chip, the replica-casted MESIF piece was cut into parts of approximately 18 × 10 × 3 mm^3 that fit into a PDMS housing, which was fabricated using a corresponding casting mold (Figure S2). The PDMS housing structure includes a reservoir above the empty space for fitting the MESIF matrix piece, into which nutrient medium or substrates will later be placed. After fitting the MESIF piece,

https://doi.org/10.1021/acsami.2c15470
ACS Appl. Mater. Interfaces 2022, 14, 49592−49603

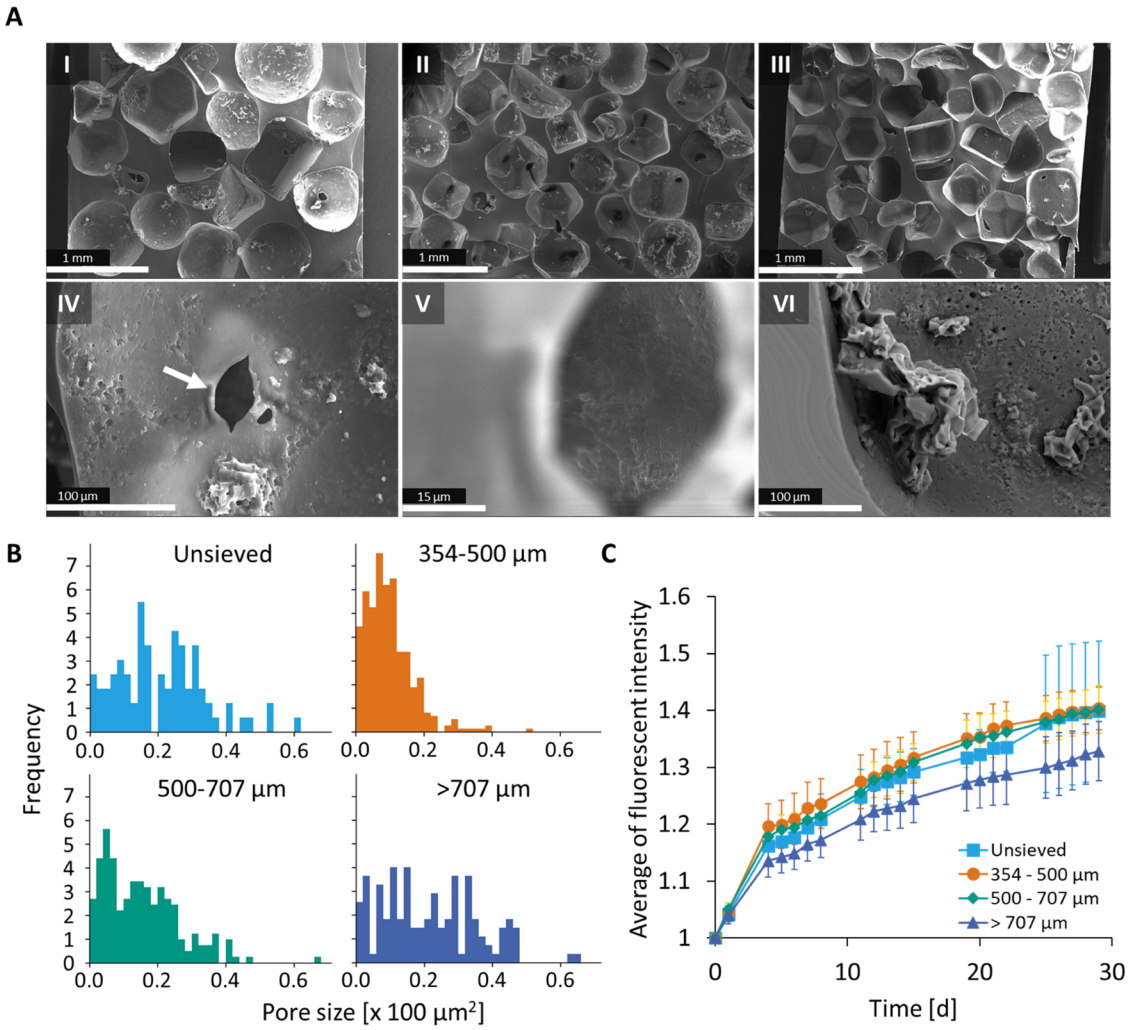

Figure 2. Morphology and diffusion properties of MESIF materials. (A) Electron micrographs of the MESIF material. Cross section of a MESIF prepared with salt crystals of >707 μm (I), 0−354 μm (II) size fractions, and unsieved table salt (III). Open connection between two pores indicated by a white arrow (IV), with zoom-in through the opening to show the back pore (V). Close up on the surface morphology of the pores reveals PDMS structures on the pore surface (VI). (B) Pore size distribution of MESIF materials prepared with porogens of variable grain size, as determined from ESEM micrographs. (C) Influence of different pore sizes on the diffusion behavior of the model solute 5-carboxyfluorescein (10 μM), applied as a drop to the environmental contact in the MESIF chip. The curves, obtained by automated fluorescence image analysis as detailed in Figure S3, show the increase in fluorescence over the total area of the chip with time. Note that a small pore size leads to slightly faster diffusion. Error bars are standard deviations of three independent chips.

the housing was closed with a lid, which was previously cast from PDMS and into which the holes for contact with the environment were manually punched. For assembly, the three parts of the chip (MESIF matrix piece, PDMS housing, and cover lid) were individually activated by plasma treatment and then assembled into a chip that was cured at 90 °C for 30 min for permanent bonding. For a detailed description, see Figure S2.

The workflow described here is simple and robust, could be learned by student assistants within a day, and could be used to produce ∼20 MESIF chips per day per person. The procedure developed in the course of academic research should be easily scalable to industrial formats through automation.

3.2. Physical Characterization of MESIF Materials. To gain insight into the physical properties of the MESIF matrix materials, we first analyzed the grain sizes of the porogen used, commercial table salt. For this purpose, the distribution of grain sizes was determined by dividing the salt into the respective grain sizes using a sieve with interchangeable sieve trays. The inserts used had pore sizes of 707, 500, 354, 250, and 177 μm. The masses of the respective size fractions of the sieve analysis and the percentage share of the total mass of the sieved salt were determined (Figure S7). The fractions 707−500 and 500−354 μm showed the largest mass fraction with together almost 80%. Sufficient amounts of salt crystals were obtained from the >707, 707−500, 500−354, and 354−250 μm salt fractions to prepare materials and perform further analysis of MESIF pore sizes, diffusion, and growth behavior with model organisms.

To visualize the pore structure and morphology within MESIF, thin film sections were cut, coated with platinum, and examined using ESEM. Figure 2A shows representative ESEM images of MESIF prepared with different porogen grain sizes. The images show a stochastic arrangement of pores characterized by different shapes reflecting the morphology of salt crystals. At high magnification, many pores show sharp-edged cracks in the pore surface at their contact surfaces (Figure 2A(IV)) through which the pore behind can be seen

https://doi.org/10.1021/acsami.2c15470
ACS Appl. Mater. Interfaces 2022, 14, 49592−49603

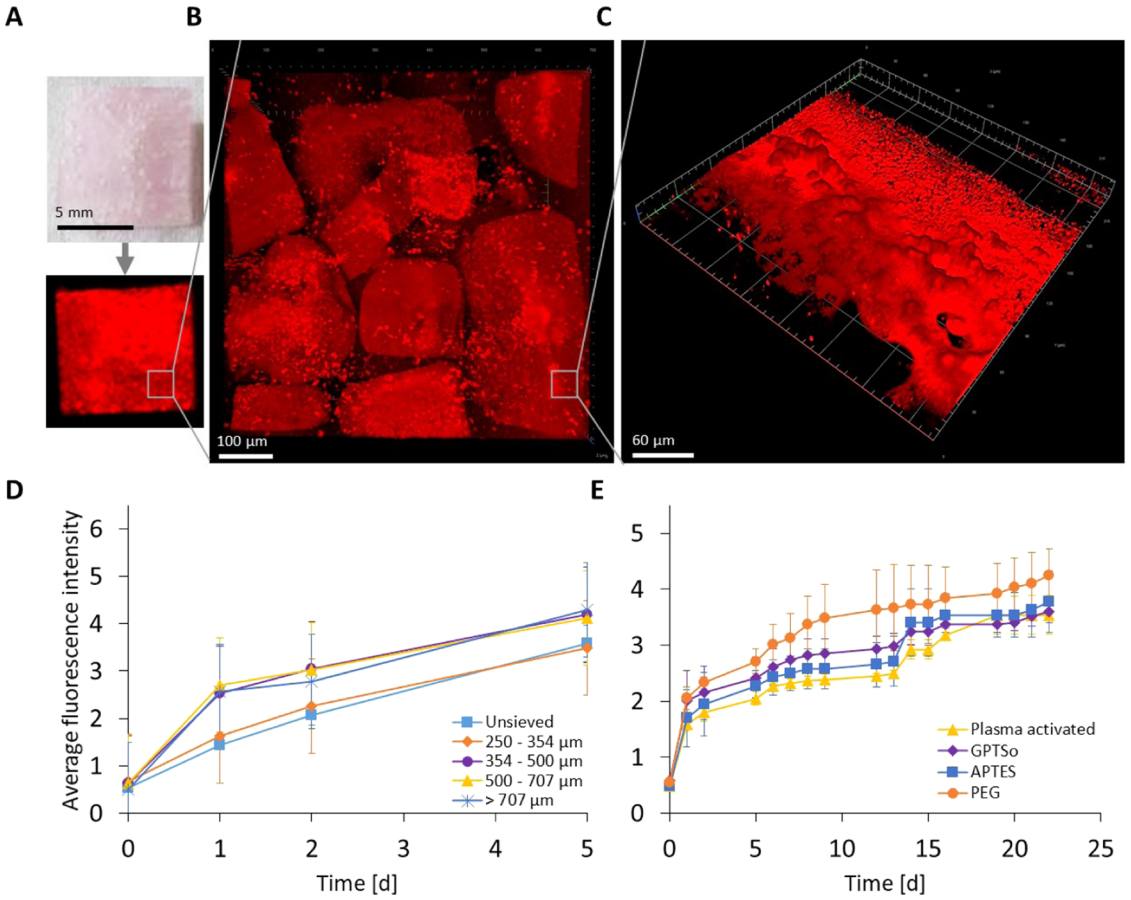

Figure 3. Growth of *E. coli* cells expressing the red fluorescent protein (*E. coli*-RFP) in MESIF chips. (A) Daylight (top) and fluorescence (bottom) photographs of MESIF inoculated with *E. coli*-RFP. (B) Confocal micrograph of the MESIF microstructure showing three-dimensional interconnected pores filled with *E. coli*-RFP. (C) Magnified micrograph showing cells that grow in dense populations and biofilms. (D) Effect of different pore sizes on the growth behavior. *E. coli*-RFP was inoculated into the environmental contact of the MESIF chip and incubated at 37 °C for several days. The time course of growth was determined by the increase in fluorescence intensity over the entire area of the chip. Note that larger pore sizes (yellow, purple) result in a slightly increased spreading velocity of cells in the matrix. (E) Influence of the surface modification of MESIF prepared with 500−707 μm porogen on the growth behavior. Note that the presence of PEG groups appears to promote faster spreading of *E. coli*-RFP inside the chip. Error bars in panels (D) and (E) are standard deviations of three independent chips.

when focused further (Figure 2A(V)). Also, thin, crumpled PDMS pieces are found in some pores (Figure 2A(VI)). These optical findings suggest that the interconnecting cracks between individual pores are formed in the course of porogen leaching, resulting in interconnectivity between the pores.

ESEM images were also used to determine the pore size distribution of the two-dimensional pore cross sections of the sponges using ImageJ analysis[24] (Figure 2B). The histograms show absolute pore sizes smaller than the experimentally determined porogen particle sizes (Figure S7) because only a two-dimensional section of the three-dimensional MESIF material was recorded in the ESEM and thus the pores were not imaged in their maximum cross-sectional area depending on the position of the section. Despite this systematic error, it is visible that with larger salt crystals, the pore size distribution becomes progressively wider and flatter. In contrast, smaller salt crystals produce narrower and steeper distributions. The pore size distribution of the unsieved salt shows a superposition of the distributions of all size fractions.

To confirm homogeneous interconnectivity of the pores in the MESIF matrix, diffusion studies were then performed using the fluorescent dye 5-carboxyfluorescein as a model solute (Figure 2C). An automated evaluation of fluorescence images of MESIF chips was developed to follow the course of dissociation of a fluorophore solution applied to the contact hole into the three-dimensional matrix (Figure S3). On the one hand, this method revealed that the fluorophore spreads almost homogeneously throughout the matrix. On the other hand, the method could be used to quantify differences of the matrix on the dissociation of the solute and also migration of fluorescently labeled model organisms. As an example, it is shown in Figure 2C that the pore sizes of the MESIF matrix have little effect on the passive diffusion of the fluorescent solute. However, the trend was evident that smaller pore sizes lead to faster diffusion, presumably due to higher capillary forces in the smaller pores. It should be noted that, in principle, smaller porogen sizes than the particle fractions used here can also be applied for the preparation of MESIF. Since particle sizes <177 μm were rare in the salt batch (Figure S7), this fraction was not included in our study to investigate its influence on pore size, diffusion behavior, and bacterial colonization.

We also tested the modifiability of the surface of the MESIF matrix using organosilane-based chemistry. To this end, either primary amino or hydroxyl groups or hydrophilic PEG moieties were installed on the surface of the MESIF matrix

https://doi.org/10.1021/acsami.2c15470
ACS Appl. Mater. Interfaces 2022, 14, 49592−49603

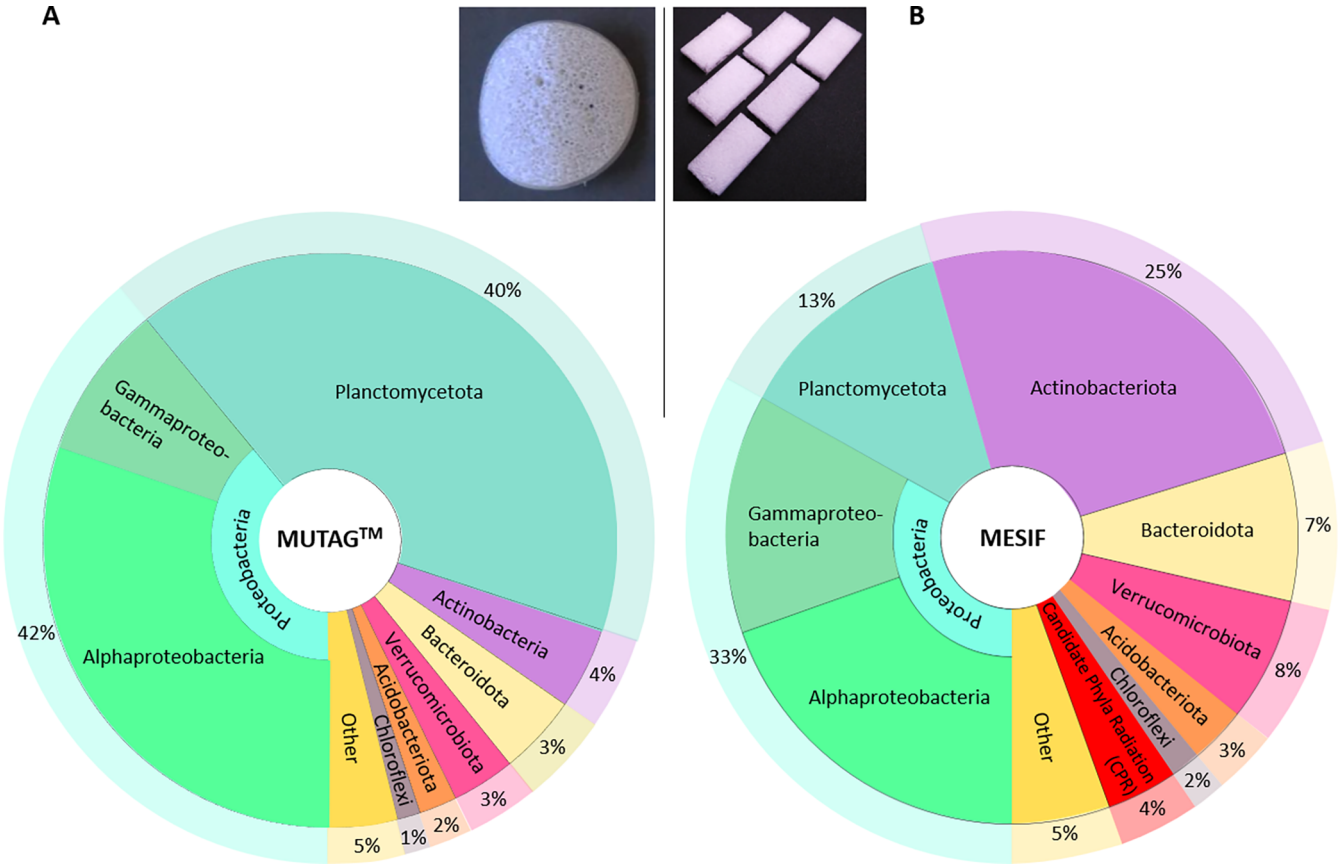

Figure 4. Phylogenetic distribution of microorganisms in a moving bed biofilter of a fish farm. Shown are KRONA charts of a 16S rRNA amplicon analysis of microorganisms that grew on a commercial biofilm support MUTAG BioChip (A) or MESIF (B). Both carriers were incubated for 18 days in the biofilter of a commercial aquaculture facility, the latter (B) showing a significantly higher biodiversity.

using APTES, GPTS trimethoxysilane with subsequent hydrolytic opening of the epoxy group, or a PDMS-PEG block copolymer, respectively.

For chemical structures and detailed modification protocols, see Figure S4 and the Section 2. The successful chemical modification of the surface was confirmed by water contact angle measurements (Figure S8). In the course of these studies, we also demonstrated that even large functional macromolecules, such as DNA oligonucleotides, can be efficiently installed on the surface of the MESIF matrix (Figure S5). Using the model solute 5-carboxyfluorescein, we could demonstrate that surface modification with functional groups, such as amino-, hydroxyl-, or PEG groups significantly affects the passive diffusional transport of small molecules through the MESIF matrix (Figure S9). We note that such surface modifications can be used to influence the colonization of MESIF surfaces by different bacterial communities, as it is well known that the colonization of surfaces can be strongly influenced by their polarity, hydrophobicity, and micro- and nanotopography.[25,26]

3.3. Bacterial Growth Studies. We then investigated the growth of model bacteria in MESIF materials using genetically modified *E. coli* cells intracellularly expressing the red fluorescent protein (*E. coli*-RFP). To obtain quantitative data, growth experiments were performed in chips with different pore sizes as well as different surface modifications, analogous to the diffusion experiments described above (Figure 2C). For this purpose, 20 μL of *E. coli*-RFP preculture ($OD_{600} \sim 3$) in LB medium was pipetted onto the contact hole of the chips, which were previously saturated with LB medium. The inoculated chips were placed in Petri dishes and the dishes were sealed and incubated at 37 °C for up to 22 days. The propagation of the fluorescence signal over the entire chip area was documented by imaging.

After only 2 days, the growth of fluorescent bacteria was visible to the naked eye as a pink coloration of the material (Figure 3A, see also Figure S10). Confocal microscopy imaging revealed the MESIF microstructure, which showed three-dimensional interconnected pores filled with *E. coli*-RFP (Figure 3B). Magnified micrographs inside a pore showed cells growing in dense populations and biofilms (Figure 3C).

Quantitative assessment of the *E. coli*-RFP growth in the MESIF chips revealed that larger pore sizes led to a slightly faster cell migration inside the MESIF matrix (Figure 3D). The influence of MESIF surface modifications on the growth behavior of *E. coli*-RFP was also investigated (Figure 3E). The results suggested that modification with PEG groups led to faster spreading of these *E. coli* cells within the MESIF matrix.

Although the fluorescence-based growth observations shown here are very useful for quantitative assessment under laboratory conditions, this approach is unsuitable for real-world applications in the field because microorganisms rarely exhibit strong autofluorescence signals and often display very slow reproduction times. It is therefore of great interest that fluorescence-independent detection of microbial colonization of MESIF chips is possible in a straightforward manner. MESIF materials show altered turbidity and opacity due to microbial colonization, which can be detected very easily by UV

https://doi.org/10.1021/acsami.2c15470
ACS Appl. Mater. Interfaces 2022, 14, 49592−49603

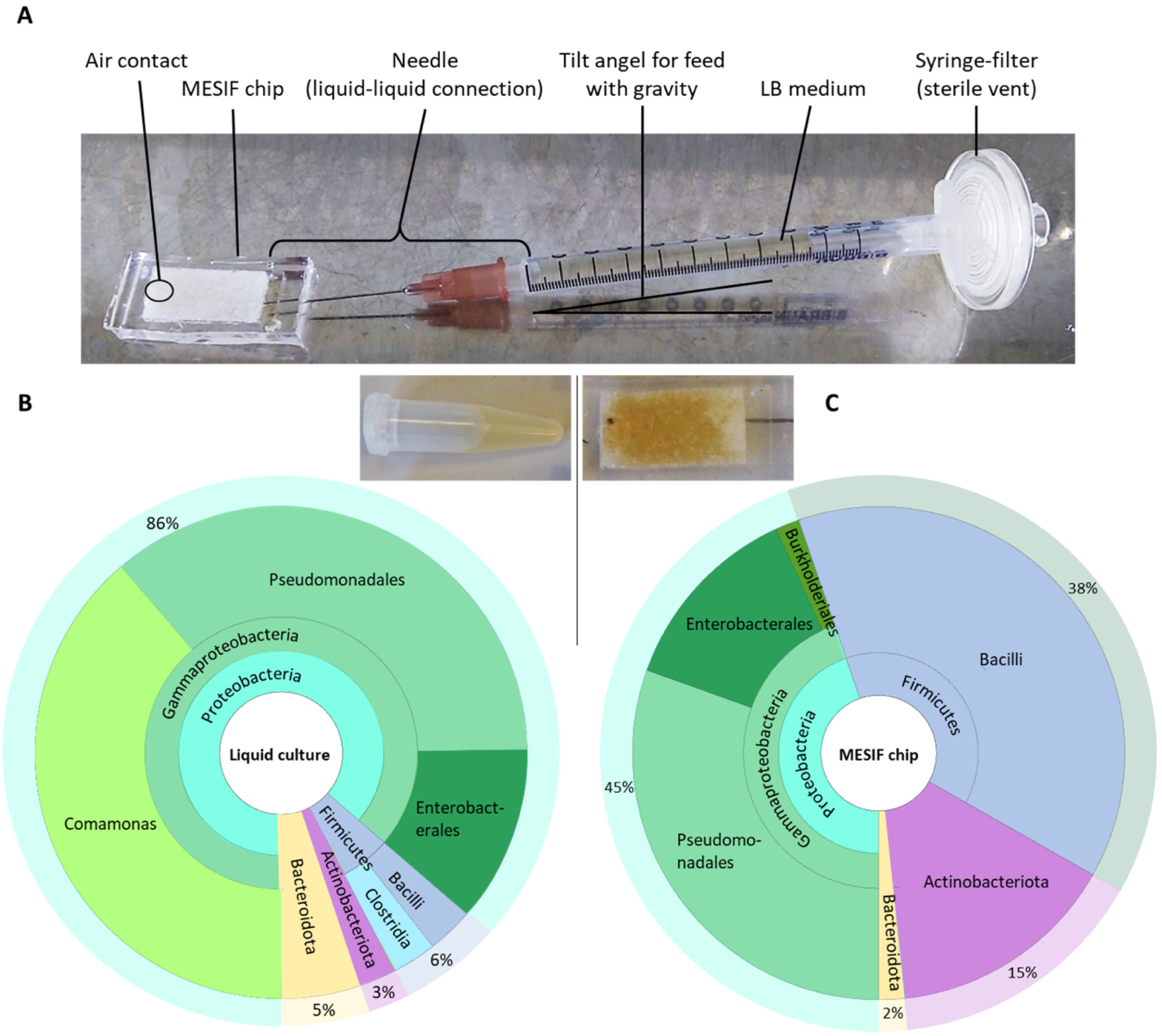

Figure 5. Phylogenetic distribution of airborne microorganisms from a poultry farm environment: (A) reservoir feature of the MESIF chip was connect for continuous supply of sterile cultivation medium. (B, C) KRONA charts of the 16S rRNA amplicon sequencing analysis of microorganisms that were allowed to grow for 9 days in open control tubes filled with LB media (B) or the MESIF chip (C). Note that the MESIF chip-based sampling led to a higher biodiversity and was able to enrich the biotechnologically relevant group of *Actinobacteriota* by 5-fold as compared to the liquid medium.

transillumination. Hereby, using the example of the very slow growing *Bacillus marisflavi*, it was shown that the growth can be monitored in real time with a normal webcam and used to quantify the biomass in the MESIF chip (Figure S11). This property of the MESIF material is thus extremely useful, for example, to quickly assess in the field whether successful colonization of the matrix and thus successful sampling of a habitat has occurred.

3.4. Sampling of Microbial Communities from a Moving Bed Biofilter. Having investigated the physical properties of the MESIF material and demonstrated its basic suitability for culturing bacteria, we now wanted to test whether the MESIF chip is indeed suitable for enriching complex microbial communities from natural habitats. For this purpose, we initially chose an aerobic moving bed biofilter of a fish farm where adult pikeperch are kept at a stocking density of ~15 kg m^{-3}. To evaluate the performance of the MESIF material, we used commercially available polyethylene biofilter carrier chips (MUTAG BioChips), which are reported by the manufacturer to have a high protected active surface area of more than 5500 m^2 m^{-3} and are often used as biocarriers for moving bed biofilm reactor studies.[27,28] Untreated pieces of MESIF and MUTAG chips were incubated free-floating in the biofilter tank for 18 days, then collected, briefly washed with deionized water, and frozen at −20 °C for temporary storage and transport. gDNA was extracted from the chips using commercially available extraction kits according to the manufacturer's protocol, and the amount of extracted gDNA was quantified photometrically. Characterization of the obtained gDNA was done by gel electrophoresis and 16S rRNA amplicon sequencing (Figure S6; for details, see also the Section 2). The quality of the extracted gDNA was sufficiently

https://doi.org/10.1021/acsami.2c15470
ACS Appl. Mater. Interfaces 2022, 14, 49592−49603

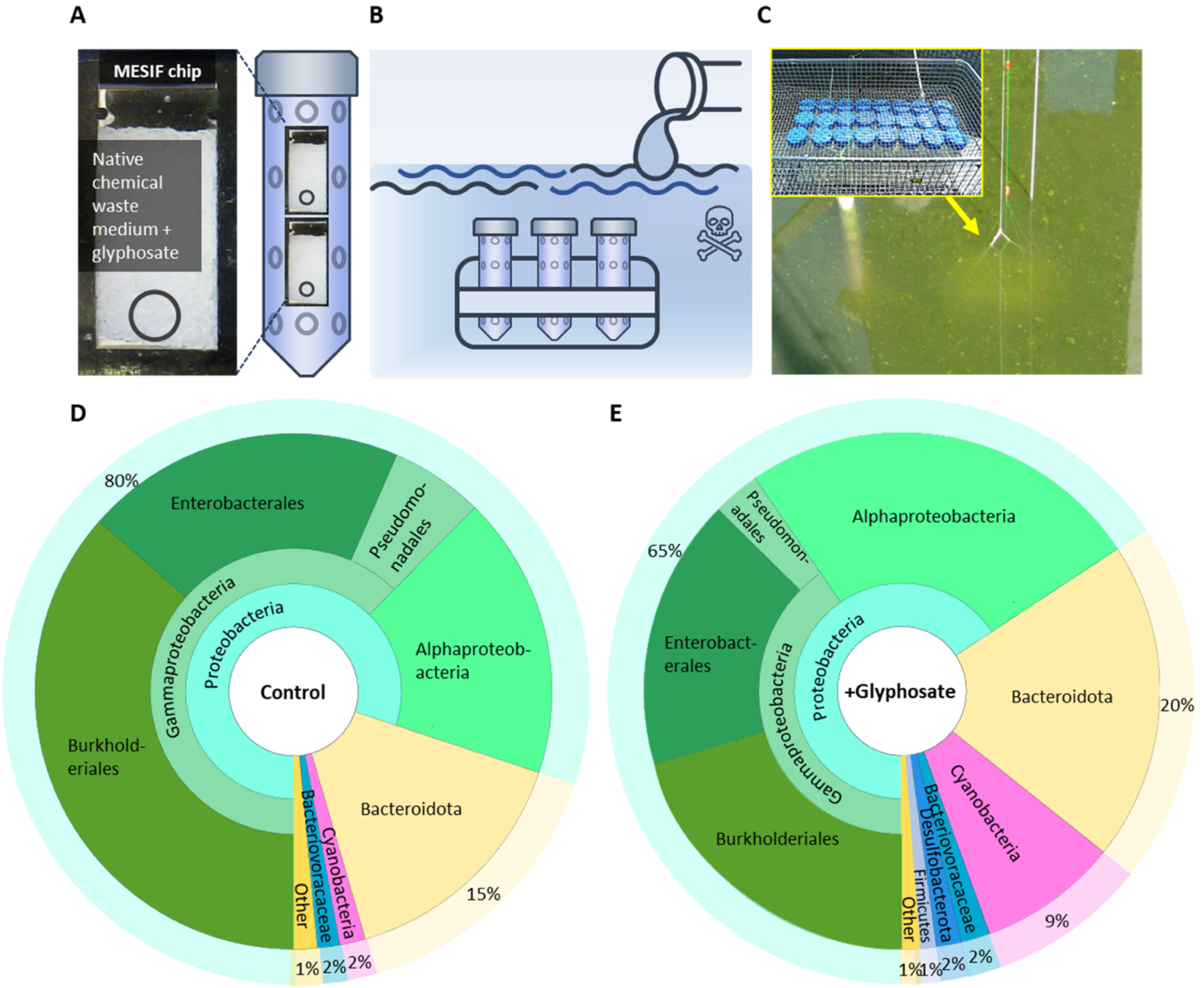

Figure 6. Targeted enrichment and sampling of microorganisms from a chemical WWTP under glyphosate selection. The MESIF chip's reservoir was filled with a sterilized native WWTP medium supplemented with 8 g L^{-1} glyphosate or pure sterilized WWTP medium as control. (A) Two chips were packed into a 50 mL Falcon tube equipped with handmade openings to allow inflow of WWTP effluent (gray circles, in panel A). The Falcon tubes were fixed in a metal rack and immersed ~40 cm deep in the static chemical wastewater collection tank in the open air (B, C) and left for 6 days. (D, E) KRONA charts of the 16S amplicon sequencing analysis of microorganisms that were collected from the control (D) or glyphosate (E) MESIF chips. Note that the glyphosate-based sampling led to an enrichment of *Desulfobacteria*, *Firmicutes* as well as a substantial larger fraction of *Cyanobacteria*.

high to produce a sequencing library for Illumina sequencing using commercially available kits.

Following Illumina 16S rRNA amplicon sequencing, the sequences found were bioinformatically processed, analyzed, and visualized in KRONA charts (for details, see the Section 2). The resulting KRONA charts in Figure 4 illustrate that the microbial community on the MUTAG carrier is strongly dominated by *Alphaproteobacteria* and *Planctomycetes*, the latter being especially known to form biofilms on various surfaces.[29] In contrast, the MESIF material showed a much broader distribution of different bacterial species. Notably, in the MESIF chip, species from the so-called *Candidate Phyla Radiation* (CPR)[30] could be enriched. Based on cultivation-independent approaches, such as 16S rRNA amplicon sequencing, metagenomics, and single-cell genomics,[31] it is currently assumed that this taxon comprises about 70% of the microbial dark matter.[2] Many CPR genomes seem to lack ubiquitous biosynthetic pathways, e.g., for the production of amino acids, nucleotides, cofactors, and membrane lipids, while protein families associated with cell−cell interactions are frequently found in this group.[32,33] Moreover, some CPRs seem to live in symbiotic relationships, which could also be the reason why they are so difficult to culture and still very poorly studied.[2] With this in mind, the initial sampling experiments with the MESIF chips seem very exciting and give hope that further studies and facilitated recovery of isolates may shed light on this enigmatic taxon.

3.5. Sampling of Airborne Microbial Communities. To test real-life applicability of MESIF chips for environmental issues, we then wanted to investigate whether sampling of airborne microbial communities was possible. For this purpose, the designed reservoir feature of the MESIF chip was exploited to provide a continuous supply of a cultivation medium (LB) to the porous interior of the chip to enable for a long

https://doi.org/10.1021/acsami.2c15470
ACS Appl. Mater. Interfaces 2022, 14, 49592−49603

incubation period in a dry environment (Figure 5A). Specifically, the reservoir was filled with LB medium and connected via a cannula to a syringe sealed with a sterile filter. In this simple setup, the syringe serves as a sterile aerated fluid reservoir from which the loss of moisture in the MESIF matrix—due to evaporation at the environmental contact—is continuously replenished as the matrix acts as a capillary pump. Indeed, we had previously verified that the MESIF matrix acts as an efficient capillary pump due to the large number of interconnected microcavities (Figure S12). For comparison of the sampling of airborne microbial communities, open 1.5 mL Eppendorf tubes containing the same LB media were used. Triplicates of both sampling devices were incubated for 9 days in an open interior of a poultry farm with a stocking density of 2 chickens per m^2.

Genomic DNA was extracted and 16S rRNA amplicon sequencing and bioinformatic analysis were conducted as described above. While the liquid culture showed a complete overgrowth of *Proteobacteria* (Figure 5B), representing 86% of the total abundance, the MESIF chip enabled the isolation of a much more evenly distributed composition of airborne microorganisms, particularly *Proteobacteria*, *Firmicutes*, and *Actinobacteriota*. The latter taxonomic group is particularly interesting because of its ability to produce specific secondary metabolites such as anticancer, antifungal, and immunosuppressive agents. Thus, two-third of all known antibiotics are currently produced by *Actinobacteriota*, which are therefore of great medical and biotechnological interest.[34,35] Further studies with the MESIF chip could lead to the isolation of more species from this important group and to better exploit its biotechnological potential. Also, the broad distribution of different microorganisms on the MESIF chip shows very clearly that the simple and pragmatic reservoir concept presented here is very well suited to sample complex airborne habitats, even when using a nonoptimal medium such as LB, which should rather favor the enrichment of well-culturable organisms. Since the MESIF matrix and reservoir can be loaded with a variety of substances, this approach should also be applicable for targeted enrichment of microorganisms, for example, by filling the reservoir with a chemical substance that attracts or repels specific microorganisms.

3.6. Targeted Enrichment of Microbial Communities from a Wastewater Treatment Plant. To demonstrate that the MESIF chip is applicable for selective enrichment of microbial communities when the reservoir is filled with a specific chemical, we then conducted sampling studies in the highly challenging wet habitat of a WWTP. For this purpose, we aimed at the possible selective enrichment of microorganisms using the herbicide glyphosate, which is a phosphonic acid compound and is used as the biologically active major component of some broad-spectrum or total herbicides on a million-ton scale worldwide.[36] To enable sampling, the reservoir of the MESIF chip was filled with a sterilized native WWTP medium supplemented with 8 g L^{-1} glyphosate. Chips whose reservoirs were filled with sterilized WWTP medium only were used as controls. Two chips loaded with either glyphosate or the control medium were packed into a 50 mL Falcon tube in which the handmade openings allow inflow of WWTP effluent (Figure 6A). The Falcon tubes loaded in this manner were fixed in a metal rack and then immersed ∼40 cm deep in a static chemical wastewater collection tank of the waste management system of the Karlsruhe Institute of Technology in the open air (Figure 6B,C) and left for 6 days.

Isolation of gDNA, 16S rRNA amplicon sequencing, and bioinformatic analysis were conducted as described above. The KRONA chart shows that the MESIF control chip lacking glyphosate showed mainly different *Proteobacteria* as well as some *Bacteroidota* and a small amount of *Cyanobacteria* and *Bacteriovoracaceae*. In contrast, the glyphosate-containing MESIF chip showed an almost 5-fold larger fraction of *Cyanobacteria*, suggesting their enrichment due to the presence of glyphosate. Furthermore, the phyla *Desulfobacterota* and *Firmicutes* could be found in the glyphosate MESIF chip. The occurrence of *Desulfobacterota* is especially interesting since anaerobic sulfate or sulfur-reducing bacteria in this phylum have been described to utilize organic acids,[37] which could be a metabolic product of the glyphosate degradation of other bacteria in the sample. The first steps in the degradation of glyphosate in bacteria involve the conversion of glyphosate into the weak organic acid aminomethylphosphonic acid through the glyphosate oxidoreductase.[38] The acid can then be excreted into the environment or cleaved into other molecules. The presence of *Desulfobacterota* in the MESIF chip containing glyphosate could thus indicate that the resulting aminomethylphosphonic acid of the herbicide degradation may be consumed by *Desulfobacterota*.

We also analyzed the data regarding the presence of known glyphosate-degrading organisms by aligning all amplicon sequences from the chip against the total genomes of three organisms known for their glyphosate degradation: *Enterobacter* sp. *E*20,[39] *Pseudomonas azotoformans*,[40] and *Comamonas odontotermitis*.[41] Only in case of the glyphosate-containing MESIF chip, more than 100 amplicons could be matched to different sequences within the 16S rRNA genes of the three mentioned organisms. The same procedure performed for the amplicons from the MESIF chip lacking glyphosate, amplicons could only be matched to sequences that were found for *Enterobacter* sp. *E*20 but not the other two organisms. These results are a strong indication that the MESIF chip with its reservoir is a very well suited platform for the targeted enrichment of microorganisms. In the future, further metagenomics analyses will be performed to explore the glyphosate degradation pathways in the chips in detail. Since initial preliminary tests likewise suggest that the MESIF chip is also suitable for sampling soil (Figure S13), we expect that the approach described here will enable a variety of studies to elucidate microbial dark matter.

4. CONCLUSIONS

In summary, here, we reported the fabrication and application of a novel macroporous silicone chip. Although research on PDMS foams has been long standing,[22] the suitability of these low-cost, bioinert, and diversely modifiable materials for targeted bacterial enrichment has not been systematically investigated. Integrating these macroporous elastomeric silicone foam (MESIF) materials into an easily fabricated and scalable chip design results in an ideal device for hunting microbial dark matter. Thus, here, we demonstrate in initial proof-of-concept applications the use of MESIF chips for sampling diverse habitats ranging from turbulent wet to dry air-based environments. All growth and sampling results consistently show that the MESIF chips are not only practical to use for such analyses with high robustness, but that the material also provides detectability of a broad cross section of

https://doi.org/10.1021/acsami.2c15470
ACS Appl. Mater. Interfaces 2022, 14, 49592−49603

microorganisms present in the habitat in a short time of a few days. We caution that the results shown here are only proof-of-concept in nature. However, we anticipate that our approach will pave the way for systematic sampling studies to contribute to the identification of microbial dark matter by varying the material properties of the MESIF, as well as to develop new approaches for the cultivation and exploitation of previously unculturable microorganisms using the reservoir concept of our chips.

■ ASSOCIATED CONTENT

Supporting Information

The Supporting Information is available free of charge at https://pubs.acs.org/doi/10.1021/acsami.2c15470.

Detailed workflow of the MESIF material preparation (Figure S1); workflow of the MESIF chip assembly (Figure S2); automated evaluation of fluorescence images of MESIF chips (Figure S3); structural formulae of the surface modification applied to MESIF materials (Figure S4); installation of DNA oligonucleotides on the surface of the MESIF matrix (Figure S5); representative workflow for DNA extraction from MESIF chips (Figure S6); distribution of grain sizes as determined by sieve analysis (Figure S7); water contact angle measurements to confirm the successful chemical modification of the MESIF surfaces (Figure S8); influence of different surface modifications on the diffusion behavior of 5-carboxyfluorescein in MESIF chips (Figure S9); images of MESIF chips with different pore sizes 2 days after inoculation with *E. coli*-RFP (Figure S10); evaluation of nonfluorescent microbial growth in MESIF chips (Figure S11); MESIF matrix acts as a capillary pump (Figure S12); and microbial sampling from soil environment (Figure S13) (PDF)

Real-time imaging of microbial growth in a MESIF chip (Movie M1) (AVI)

■ AUTHOR INFORMATION

Corresponding Author

Christof M. Niemeyer − *Institute for Biological Interfaces 1 (IBG-1), Biomolecular Micro- and Nanostructures, Karlsruhe Institute of Technology (KIT), D-76344 Eggenstein-Leopoldshafen, Germany;* orcid.org/0000-0002-8837-081X; Email: niemeyer@kit.edu

Authors

Ahmed E. Zoheir − *Institute for Biological Interfaces 1 (IBG-1), Biomolecular Micro- and Nanostructures, Karlsruhe Institute of Technology (KIT), D-76344 Eggenstein-Leopoldshafen, Germany; Biotechnology Research Institute, Department of Genetics and Cytology, National Research Centre (NRC), 12622 Cairo, Egypt;* orcid.org/0000-0001-5656-2932

Laura Meisch − *Institute for Biological Interfaces 1 (IBG-1), Biomolecular Micro- and Nanostructures, Karlsruhe Institute of Technology (KIT), D-76344 Eggenstein-Leopoldshafen, Germany*

Marta Velaz Martín − *Institute for Biological Interfaces 1 (IBG-1), Biomolecular Micro- and Nanostructures, Karlsruhe Institute of Technology (KIT), D-76344 Eggenstein-Leopoldshafen, Germany*

Christoph Bickmann − *Institute for Biological Interfaces 1 (IBG-1), Biomolecular Micro- and Nanostructures, Karlsruhe Institute of Technology (KIT), D-76344 Eggenstein-Leopoldshafen, Germany*

Alexei Kiselev − *Institute of Meteorology and Climate Research, Department of Atmospheric Aerosol Research (IMK-AAF), Karlsruhe Institute of Technology (KIT), D-76344 Eggenstein-Leopoldshafen, Germany*

Florian Lenk − *Institute for Biological Interfaces 5 (IBG-5), Biotechnology and Microbial Genetics, Karlsruhe Institute of Technology (KIT), D-76344 Karlsruhe, Germany*

Anne-Kristin Kaster − *Institute for Biological Interfaces 5 (IBG-5), Biotechnology and Microbial Genetics, Karlsruhe Institute of Technology (KIT), D-76344 Karlsruhe, Germany*

Kersten S. Rabe − *Institute for Biological Interfaces 1 (IBG-1), Biomolecular Micro- and Nanostructures, Karlsruhe Institute of Technology (KIT), D-76344 Eggenstein-Leopoldshafen, Germany;* orcid.org/0000-0001-7909-8191

Complete contact information is available at: https://pubs.acs.org/10.1021/acsami.2c15470

Notes

The authors declare the following competing financial interest(s): The authors declare that a patent application has been filed. A.E.Z., K.S.R and C.M.N. declare that they have a competing interest.

■ ACKNOWLEDGMENTS

This work was supported through the Helmholtz program "Materials Systems Engineering" under the topic "Adaptive and Bioinstructive Materials Systems". The authors acknowledge funding through KIT EXU project DigiteLiSE and Bundesministerium für Bildung und Forschung (BMBF, project 161L0284A MicroMatrix). The authors thank Theresa Haag, Johannes Reith (IBG-1), and David Thiele (IBG-5) for experimental help, Denis Kapieske and Kai Meissner (Acheron GmbH, Bremen) for providing biofilter samples, and Tawheed Hashem for facilitating sampling in the poultry farm.

■ REFERENCES

(1) Rinke, C.; Schwientek, P.; Sczyrba, A.; Ivanova, N. N.; Anderson, I. J.; Cheng, J.-F.; Darling, A.; Malfatti, S.; Swan, B. K.; Gies, E. A.; Dodsworth, J. A.; Hedlund, B. P.; Tsiamis, G.; Sievert, S. M.; Liu, W.-T.; Eisen, J. A.; Hallam, S. J.; Kyrpides, N. C.; Stepanauskas, R.; Rubin, E. M.; Hugenholtz, P.; Woyke, T. Insights into the Phylogeny and Coding Potential of Microbial Dark Matter. *Nature* **2013**, *499*, 431−437.

(2) Hug, L. A.; Baker, B. J.; Anantharaman, K.; Brown, C. T.; Probst, A. J.; Castelle, C. J.; Butterfield, C. N.; Hernsdorf, A. W.; Amano, Y.; Ise, K.; Suzuki, Y.; Dudek, N.; Relman, D. A.; Finstad, K. M.; Amundson, R.; Thomas, B. C.; Banfield, J. F. A New View of The Tree of Life. *Nat. Microbiol.* **2016**, *1*, 16048.

(3) Hall-Stoodley, L.; Costerton, J. W.; Stoodley, P. Bacterial Biofilms: From the Natural Environment to Infectious Diseases. *Nat. Rev. Microbiol.* **2004**, *2*, 95−108.

(4) Verstraete, W. The Manufacturing Microbe. *Microb. Biotechnol.* **2015**, *8*, 36−37.

(5) Lewis, W. H.; Tahon, G.; Geesink, P.; Sousa, D. Z.; Ettema, T. J. G. Innovations to Culturing the Uncultured Microbial Majority. *Nat. Rev. Microbiol.* **2021**, *19*, 225−240.

(6) Berdy, B.; Spoering, A. L.; Ling, L. L.; Epstein, S. S. *In situ* Cultivation of Previously Uncultivable Microorganisms Using the Ichip. *Nat. Protoc.* **2017**, *12*, 2232−2242.

(7) Grösche, M.; Zoheir, A. E.; Stegmaier, J.; Mikut, R.; Mager, D.; Korvink, J. G.; Rabe, K. S.; Niemeyer, C. M. Microfluidic Chips for Life Sciences-A Comparison of Low Entry Manufacturing Technologies. *Small* **2019**, *15*, No. e1901956.
(8) Sui, G.; Wang, J.; Lee, C.-C.; Lu, W.; Lee, S. P.; Leyton, J. V.; Wu, A. M.; Tseng, H.-R. Solution-Phase Surface Modification in Intact Poly(dimethylsiloxane) Microfluidic Channels. *Anal. Chem.* **2006**, *78*, 5543−5551.
(9) Yu, Q.; Zhang, Y.; Chen, H.; Wu, Z.; Huang, H.; Cheng, C. Protein Adsorption on Poly(N-Isopropylacrylamide)-Modified Silicon Surfaces: Effects of Grafted Layer Thickness and Protein Size. *Colloids Surf., B* **2010**, *76*, 468−474.
(10) Bolger, A. M.; Lohse, M.; Usadel, B. Trimmomatic: A Flexible Trimmer for Illumina Sequence Data. *Bioinformatics* **2014**, *30*, 2114−20.
(11) Martin, M. Cutadapt Removes Adapter Sequences from High-Throughput Sequencing Reads. *EMBnet. J.* **2011**, *17*, 10−12.
(12) Bushnell, B. BBMap. https://sourceforge.net/projects/bbmap/. (accessed Apr 2022).
(13) Magoc, T.; Salzberg, S. L. FLASH: Fast Length Adjustment of Short Reads to Improve Genome Assemblies. *Bioinformatics* **2011**, *27*, 2957−63.
(14) Rognes, T.; Flouri, T.; Nichols, B.; Quince, C.; Mahe, F. VSEARCH: A Versatile Open Source Tool for Metagenomics. *PeerJ.* **2016**, *4*, No. e2584.
(15) Pruesse, E.; Peplies, J.; Glockner, F. O. SINA: Accurate High-Throughput Multiple Sequence Alignment of Ribosomal RNA Genes. *Bioinformatics* **2012**, *28*, 1823−1829.
(16) Ondov, B. D.; Bergman, N. H.; Phillippy, A. M. Interactive Metagenomic Visualization in a Web Browser. *BMC Bioinf.* **2011**, *12*, 1−10.
(17) Donlan, R. M. Biofilms: Microbial Life on Surfaces. *Emerg. Infect. Dis.* **2002**, *8*, 881−890.
(18) Flemming, H. C.; Wingender, J.; Szewzyk, U.; Steinberg, P.; Rice, S. A.; Kjelleberg, S. Biofilms: An Emergent Form of Bacterial Life. *Nat. Rev. Microbiol.* **2016**, *14*, 563−75.
(19) Hansen, S. H.; Kabbeck, T.; Radtke, C. P.; Krause, S.; Krolitzki, E.; Peschke, T.; Gasmi, J.; Rabe, K. S.; Wagner, M.; Horn, H.; Hubbuch, J.; Gescher, J.; Niemeyer, C. M. Machine-Assisted Cultivation and Analysis of Biofilms. *Sci. Rep.* **2019**, *9*, No. 8933.
(20) Lemke, P.; Zoheir, A. E.; Rabe, K. S.; Niemeyer, C. M. Microfluidic Cultivation and Analysis of Productive Biofilms. *Biotechnol. Bioeng.* **2021**, *118*, 3860−3870.
(21) Zoheir, A. E.; Späth, G. P.; Niemeyer, C. M.; Rabe, K. S. Microfluidic Evolution-On-A-Chip Reveals New Mutations that Cause Antibiotic Resistance. *Small* **2021**, *17*, No. 2007166.
(22) Zhu, D.; Handschuh-Wang, S.; Zhou, X. Recent Progress in Fabrication and Application of Polydimethylsiloxane Sponges. *J. Mater. Chem. A* **2017**, *5*, 16467−16497.
(23) Vogelaar, L.; Lammertink, R. G. H.; Barsema, J. N.; Nijdam, W.; Bolhuis-Versteeg, L. A. M.; van Rijn, C. J. M.; Wessling, M. Phase Separation Micromolding: A New Generic Approach for Microstructuring Various Materials. *Small* **2005**, *1*, 645−655.
(24) Schneider, C. A.; Rasband, W. S.; Eliceiri, K. W. NIH Image to ImageJ: 25 Years of Image Analysis. *Nat. Methods* **2012**, *9*, 671−675.
(25) Dang, H.; Lovell, C. R. Microbial Surface Colonization and Biofilm Development in Marine Environments. *Microbiol. Mol. Biol. Rev.* **2016**, *80*, 91−138.
(26) Kim, T.; Kwon, S.; Lee, J.; Lee, J. S.; Kang, S. A Metallic Anti-Biofouling Surface with a Hierarchical Topography Containing Nanostructures on Curved Micro-Riblets. *Microsyst. Nanoeng.* **2022**, *8*, 1−14.
(27) Dan, N. H.; Le Luu, T. High Organic Removal of Landfill Leachate Using a Continuous Flow Sequencing Batch Biofilm Reactor (CF-SBBR) with Different Biocarriers. *Sci. Total Environ.* **2021**, *787*, No. 147680.
(28) Mazioti, A. A.; Koutsokeras, L. E.; Constantinides, G.; Vyrides, I. Untapped Potential of Moving Bed Biofilm Reactors with Different Biocarrier Types for Bilge Water Treatment: A Laboratory-Scale Study. *Water* **2021**, *13*, 1810.
(29) Wiegand, S.; Jogler, M.; Boedeker, C.; Pinto, D.; Vollmers, J.; Rivas-Marín, E.; Kohn, T.; Peeters, S. H.; Heuer, A.; Rast, P.; Oberbeckmann, S.; Bunk, B.; Jeske, O.; Meyerdierks, A.; Storesund, J. E.; Kallscheuer, N.; Lücker, S.; Lage, O. M.; Pohl, T.; Merkel, B. J.; Hornburger, P.; Müller, R.-W.; Brümmer, F.; Labrenz, M.; Spormann, A. M.; Op den Camp, H. J. M.; Overmann, J.; Amann, R.; Jetten, M. S. M.; Mascher, T.; Medema, M. H.; Devos, D. P.; Kaster, A.-K.; Øvreås, L.; Rohde, M.; Galperin, M. Y.; Jogler, C. Cultivation and Functional Characterization of 79 Planctomycetes Uncovers their Unique Biology. *Nat. Microbiol.* **2020**, *5*, 126−140.
(30) Wiegand, S.; Dam, H. T.; Riba, J.; Vollmers, J.; Kaster, A.-K. Printing Microbial Dark Matter: Using Single Cell Dispensing and Genomics to Investigate the Patescibacteria/Candidate Phyla Radiation. *Front. Microbiol.* **2021**, *12*, 1512.
(31) Kaster, A.-K.; Sobol, M. S. Microbial Single-Cell Omics: The Crux of the Matter. *Appl. Microbiol. Biotechnol.* **2020**, *104*, 8209−8220.
(32) Castelle, C. J.; Banfield, J. F. Major New Microbial Groups Expand Diversity and Alter our Understanding of the Tree of Life. *Cell* **2018**, *172*, 1181−1197.
(33) Méheust, R.; Burstein, D.; Castelle, C. J.; Banfield, J. F. The Distinction of CPR Bacteria from Other Bacteria Based on Protein Family Content. *Nat. Commun.* **2019**, *10*, No. 4173.
(34) van der Meij, A.; Worsley, S. F.; Hutchings, M. I.; van Wezel, G. P. Chemical Ecology of Antibiotic Production by Actinomycetes. *FEMS Microbiol. Rev.* **2017**, *41*, 392−416.
(35) De Simeis, D.; Serra, S. Actinomycetes: A Never-Ending Source of Bioactive Compounds—An Overview on Antibiotics Production. *Antibiotics* **2021**, *10*, 483.
(36) Richmond, M. E. Glyphosate: A Review of its Global Use, Environmental Impact, and Potential Health Effects on Humans and other Species. *J. Environ. Stud. Sci.* **2018**, *8*, 416−434.
(37) Waite, D. W.; Chuvochina, M.; Pelikan, C.; Parks, D. H.; Yilmaz, P.; Wagner, M.; Loy, A.; Naganuma, T.; Nakai, R.; Whitman, W. B.; Hahn, M. W.; Kuever, J.; Hugenholtz, P. Proposal to Reclassify the Proteobacterial Classes *Deltaproteobacteria* and *Oligoflexia*, and the Phylum *Thermodesulfobacteria* into Four Phyla Reflecting Major Functional Capabilities. *Int. J. Syst. Evol. Microbiol.* **2020**, *70*, 5972−6016.
(38) Singh, S.; Kumar, V.; Gill, J. P. K.; Datta, S.; Singh, S.; Dhaka, V.; Kapoor, D.; Wani, A. B.; Dhanjal, D. S.; Kumar, M.; Harikumar, S. L.; Singh, J. Herbicide Glyphosate: Toxicity and Microbial Degradation. *Int. J. Environ. Res. Public Health* **2020**, *17*, 7519.
(39) Cao, G.; Jia, X.; Zheng, Y. Draft Genome Sequence of Enterobacter. Sp. E20, Isolated from Glyphosate Polluted Soil, *Proceedings of the International Symposium on Agriculture, Food and Biotechnology* (ISAFB 2019); 2019.
(40) Korkmaz, V.; Yildirim, N.; Erguven, G. O.; Durmus, B.; Nuhoglu, Y. The Bioremediation of Glyphosate in Soil Media by Some Newly Isolated Bacteria: The COD, TOC Removal Efficiency and Mortality Assessment for *Daphnia magna*. *Environ. Technol. Innovation* **2021**, *22*, No. 101535.
(41) Firdous, S.; Iqbal, S.; Anwar, S. Optimization and Modeling of Glyphosate Biodegradation by a Novel *Comamonas odontotermitis* P2 through Response Surface Methodology. *Pedosphere* **2020**, *30*, 618−627.

https://doi.org/10.1021/acsami.2c15470
ACS Appl. Mater. Interfaces 2022, 14, 49592−49603